J|A|C|S
ARTICLES
Published on Web 09/04/2004

Spontaneous Gas-Phase Generation of Needle-Shaped Clusters Which Violate the Isolated Square Rule: A Facile Road to GaN Nanorods?

Alexey Y. Timoshkin*,† and Henry F. Schaefer III‡

Contribution from the Inorganic Chemistry Group, Department of Chemistry, St. Petersburg State University, University Pr. 26, Old Peterhof, St. Petersburg 198504, Russia, and Center for Computational Chemistry, University of Georgia, Athens, Georgia 30602

Received February 12, 2004; E-mail: alextim@AT11692.spb.edu

Abstract: Structures and thermodynamic properties of the imidogallanes $[HGaNH]_n$ with high oligomerization degrees $n = 7-16$ and related amido-imido compounds have been investigated theoretically at the B3LYP level of theory with all-electron pVDZ and effective core potential LANL2DZ(d,p) basis sets. Needle-shaped oligomers which violate the "isolated square rule" were found to be more stable than cage isomers. The needle-shape oligomer with $n = 16$ is predicted to be exceptionally stable at low temperatures. Octamer and hexamer clusters dominate the gas phase at higher temperatures. The highest oligomerization degree of the spontaneous cluster formation has been estimated. It is concluded that generation of the gas-phase $[HGaNH]_n$ clusters with oligomerization degree $n \geq 60$ is viable. This makes these species possible intermediates involved in the gas-phase generation of GaN nanoparticles. A case study of methyl-substituted analogues suggests that formation of the gaseous $[MeGaNH]_n$ oligomers is even more favorable compared to that of $[HGaNH]_n$. We predict that spontaneous growth of GaN oligomers is favorable thermodynamically. Laser-assisted generation of GaN nanorods at low-temperature conditions appears to be feasible.

Introduction

Group 13−15 binary compounds are prospective materials for optoelectronics and microelectronics. With modern technology moving steadily toward reducing the dimensions of operating devices, controlled synthesis of small nanosized structures with diameters in the range 1−20 nm becomes an essential task. Pickett and O'Brien emphasized in their 2001 review[1] that "reproducible routes to crystalline, stable nanoparticles still need to be established". One of the possible approaches is gas-phase particle generation using chemical vapor deposition (CVD) process. Using organometallic vapor-phase epitaxy (OMVPE) reactors, 10−20 nm GaAs clusters were generated by Sercel and co-workers as early as 1992.[2] They mentioned that "gas-phase homogeneous nucleation in OMVPE, which has been regarded until now as a troublesome parasitic reaction, may ultimately form the basis of an aerosol technology for the fabrication of novel optoelectronic devices".[3]

Formation of the group 13−15 gas-phase stable oligomers may be a good starting point (initial step) for nanoparticle generation. Among 13−15 compounds, nitrogen-containing species, in particular imido compounds, have the best potential for forming oligomers. Use of bulky substituents on the nitrogen centers allows one to isolate and structurally characterize imidometallanes with different oligomerization degrees.[4−8] In several cases, formation of polymers with $[RMNR']_n$ composition has been reported.[9−15] Both polymers and oligomers, on further heating, can be converted to group 13 nitrides.

Despite extensive studies in the condensed phase, the role of oligomers in the CVD process remains controversial. While some authors strongly oppose operation of gas-phase association reactions,[16−18] several experimental[19−28] and theoretical[29−32]

† St. Petersburg State University.
‡ University of Georgia (E-mail hfsiii@arches.uga.edu).

(1) Pickett, N. L.; O'Brien, P. *Chem. Record* **2001**, *1*, 467.
(2) Sercel, P. C.; Saunders, W. A.; Atwarter, H. A.; Vahala, K. J.; Flagan, R. C. *Appl. Phys. Lett.* **1992**, *61*, 696.
(3) Vahala, K. J.; Saunders, W. A.; Tsai, C. S.; Sercel, P. C.; Kuech, T.; Atwarter, H. A.; Flagan, R. C. *J. Vac. Sci. Technol. B* **1993**, *11*, 1660.
(4) Veith, M. *Chem. Rev.* **1990**, *90*, 3.
(5) *Chemistry of Aluminum, Gallium, Indium and Thallium*; Downs, A. J., Ed.; Chapman & Hall: New York, 1993.
(6) *Coordination Chemistry of Aluminum*; Robinson, G. H., Ed.; VCH Publishers: New York, 1993.
(7) *Comprehensive Organometallic Chemistry II*; Housecroft, C. E., Ed.; Pergamon: London, 1995; Vol. 1.
(8) *Supramolecular Organometallic Chemistry*; Haiduc, I., Eldemann, F. T., Eds.; Wiley VCH: New York, 1999.
(9) Laubengayer, A. W.; Smith, J. D.; Ehrlich, C. G. *J. Am. Chem. Soc.* **1961**, *83*, 542.
(10) Laubengayer, A. W.; Wade, K.; Lengnick, G. *Inorg. Chem.* **1962**, *1*, 632.
(11) Wiberg, E.; May, A. Z. *Naturforsch. B* **1955**, *10*, 229.
(12) Janik, J. F.; Paine, R. T. *J. Organomet. Chem.* **1993**, *449*, 39.
(13) Bähr, G. In F.I.A.T. Review of German Science, 1939−1945, *Inorganic Chemistry*, Part II, p 159, as cited in ref 42.
(14) Janik, J. F.; Wells, R. L. *Inorg. Chem.* **1997**, *36*, 4135.
(15) Jegier, J. A.; McKernan, S.; Gladfelter, W. L. *Inorg. Chem.* **1999**, *38*, 2726.
(16) Sengupta, D. *J. Phys. Chem. B* **2003**, *107*, 291.
(17) Schäfer, J.; Simons, A.; Wolfrum, J.; Fischer, R. A. *Chem. Phys. Lett.* **2000**, *319*, 477.
(18) Bergmann, U.; Reimer, V.; Atakan, B. *Phys. Chem. Chem. Phys.* **1999**, *1*, 5593.
(19) Thon, A.; Kuech, T. F. *Appl. Phys. Lett.* **1996**, *69*, 55.
(20) Safvi, S. A.; Redwing, J. M.; Tishler, M. A.; Kuech, T. F. *J. Electrochem. Soc.* **1997**, *144*, 1789.
(21) Kim, H. J.; Egashira, Y.; Komiyama, H. *Appl. Phys. Lett.* **1991**, *59*, 2521.
(22) Kim, H. J.; Egashira, Y.; Komiyama, H. *Chem. Vap. Deposition* **1992**, *1*, 20.
(23) Almond, M. J.; Drew, M. G. B.; Jenkins, C. E.; Rice, D. A. *J. Chem. Soc., Dalton Trans.* **1992**, 5.

studies suggest that gas-phase oligomers are important intermediates in AlN and GaN deposition. However, the precise chemistry and structures of the grown species are unknown.

Chemical modeling can provide insights into the gas-phase chemistry and predict the most favorable growth species. In the present report, based on a case study of a H−Ga−N−H system, we will discuss thermodynamics aspects of the gas-phase reactions, related to the gas-phase generation of nanoparticles. Despite substantial experimental studies, the detailed gas-phase chemistry involved in GaN CVD remains unclear. It is supposed[28] that the process may be described as

$$R_3Ga + NH_3 \rightarrow \underset{\text{adduct}}{R_3GaNH_3} \rightarrow \underset{\text{amido}}{[R_2GaNH_2]_3} \rightarrow [RGaNH]_n \rightarrow \underset{\text{imido}}{GaN}$$

Recently Sengupta, on the basis of the results of the DFT study of gas-phase reactions involving only *monomeric* species, speculated that since the Me_2GaNH_2 monomer concentration is low, the "ring compound is negligible and cannot initiate the main pathway for growth of GaN".[16] On the contrary, earlier theoretical studies[30] suggested that formation of *hexameric* clusters $[RGaNH]_6$, which are stable up to temperatures 920−940 K, is thermodynamically favorable for R = H, CH_3. In line with these theoretical predictions, the formation of a variety of oligomer clusters, containing up to six gallium atoms, has been confirmed by mass spectrometry in recent laser-assisted MOCVD experiments.[27] The high exothermicity of the subsequent oligomerization enthalpies ($^1/_4[MeGaNH]_4 = {}^1/_6\ [MeGaNH]_6$; $\Delta H°_{(298)} = -19$ kJ mol^{-1})[30] suggests that formation of even larger associates may be energetically favorable.

How large are the clusters that may be spontaneously formed in the gas phase? What are their most favorable *structures*? Which *conditions* (*T*, *P*) favor their formation? These are the major questions we will address in the present study.

To obtain a closed cage, the $[HGaNH]_n$ structure should possess six square and $n - 4$ hexagonal faces (where n is the oligomerization degree). In recent theoretical work devoted to oligomerization of Al analogues, $[ClAlNH]_n$[33] and $[HAlNH]_n$[34] (with n up to 10 and 15, respectively), the authors concluded that the odd-numbered structures ($n = 5, 7, 9, 11, 13, 15$) have much lower stability than the even-numbered structures ($n = 6, 8, 10, 12, 14$). Note that arbitrarily chosen structures of clusters have been constructed to obey the "isolated square rule"[35,36] found for the boron−nitrogen cages.

This rule is analogous to the "isolated pentagon rule" widely applied for fullerenes. It states that structures with isolated square faces are more stable compared to those with shared square faces. However, the widely used analogy between boron and its heavier analogues may be misleading. For example, dimerization of aromatic borazine to form D_{3d} symmetric $[HBNH]_6$ is strongly (by 290 kJ mol^{-1}) *endothermic*, while dimerization of alumazene and gallazene to form D_{3d} symmetric $[HAlNH]_6$ and $[HGaNH]_6$ is very *exothermic* (by 460 and 320 kJ mol^{-1}, respectively).[37] Substituted $C_{58}AlN$ fullerenes have more distorted structures and dimerize with twice the exothermicity of their $C_{58}BN$ analogues.[38,39] Thus, structures observed for the boron−nitrogen chemistry may not be the best choice for the heavier analogues of boron. Therefore, the validity of conclusion made by Xu, Wu, and their co-workers[33,34] about the "magic number regularity" of even-numbered clusters is questionable.

The "isolated square rule" is partially justified by the following argument. The number of square faces is always 6, and the number of hexagonal faces is $n - 4$. As n increases, the probability that an atom is bound to three square faces becomes very small. So does the probability that an atom is bound to two square faces and one hexagonal face.[40] This trend is of course true if one expands the structure in all dimensions, forming cages. However, one can imagine a series of a needle-shaped structures, obtained by the expansion in one dimension (analogous to nanotubes). The simplest possibility would be adding trimeric Ga_3N_3 rings together and capping them on both sides (Chart 1, row 1). The well-known cubic tetramer is the first member of this series, followed by the recently structurally characterized heptamer[41] and yet experimentally unknown needle-shape oligomers with $n = 10, 13, 16, ...$ The existence of such decamer structure was first proposed by Smith and co-workers.[42] Luo and Gladfelter[41] noted that the structural pattern of needle-shape oligomers is identical to that "observed for $[GaN]_3$ rings along the crystallographic c-axis of the wurtzite form of gallium nitride". Thus, these needle-shaped clusters, which have three adjacent square faces and clearly violate the "isolated square rule", emerge as a possible alternative to the cage structures. To our knowledge, such needle-shaped clusters have been not studied theoretically. Another possibility is a series of structures obtained by extension of the hexagonal prizmane with $n = 6, 10, 14, ...$ (Chart 1, row 2), proposed by Barron[43] for the isoelectronic alkylalumoxanes.

Which structures are preferred—cages or needle-shaped entities? We report here structures and thermodynamic properties for large imido compounds $[HGaNH]_n$ ($n = 7-16$). We compare the stability of needle versus cage-like structures and consider their formation under CVD conditions. The schematic pathway for their formation, possible intermediates, and their reactivity toward ammonia are also discussed.

Computational Details

All geometries were fully optimized with hybrid Hartree−Fock/density functional theory (DFT). All stationary points on the potential

(24) Egashira, Y.; Kim, H. J.; Komiyama, H. *J. Am. Ceram. Soc.* **1994**, *77*, 2009.
(25) Demchuk, A.; Porter, J.; Koplitz, B. *J. Phys. Chem. A* **1998**, *102*, 8841.
(26) Demchuk, A.; Simpson, S.; Koplitz, B. *Electrochem. Soc. Proc.* **2001**, *13*, 389.
(27) Demchuk, A.; Simpson, S.; Koplitz, B. *J. Phys. Chem. A* **2003**, *107*, 1727.
(28) Neumayer, D. A.; Ekerdt, J. G. *Chem. Mater.* **1996**, *8*, 9.
(29) Timoshkin, A. Y.; Bettinger, H. F.; Schaefer, H. F. *J. Am. Chem. Soc.* **1997**, *119*, 5668.
(30) Timoshkin, A. Y.; Bettinger, H. F.; Schaefer, H. F. *J. Phys. Chem. A* **2001**, *105*, 3249.
(31) Timoshkin, A. Y.; Bettinger, H. F.; Schaefer, H. F. *Inorg. Chem.* **2002**, *41*, 738.
(32) Kovacs, A. *Inorg. Chem.* **2002**, *41*, 3067.
(33) Xu, X.-H.; Wu, H.-S.; Zhang, F.-Q.; Zhang, C.-J.; Jin, Z.-H. *J. Mol. Struct.* **2001**, *542*, 239.
(34) Wu, H.; Zhang, C.; Xu, X.; Zhang, F.; Zhang, Q. *Chinese Sci. Bull.* **2001**, *46*, 1507.
(35) Sun, M.-L.; Slanina, Z.; Lee, S.-L. *Chem. Phys. Lett.* **1995**, *233*, 279.
(36) Fowler, P. W.; Heine, T.; Mitchell, D.; Schmidt, R.; Seifert, G. *J. Chem. Soc., Faraday Trans.* **1996**, *92*, 2197.
(37) Timoshkin, A. Y.; Frenking, G. *Inorg. Chem.* **2003**, *42*, 60.
(38) Pattanayak, J.; Kar, T.; Scheiner, S. *J. Phys. Chem. A* **2002**, *106*, 2970.
(39) Pattanayak, J.; Kar, T.; Scheiner, S. *J. Phys. Chem. A* **2003**, *107*, 4056.
(40) Zurek, E.; Woo, T. K.; Firman, T. K.; Ziegler, T. *Inorg. Chem.* **2001**, *40*, 361.
(41) Luo, B.; Gladfelter, W. L. *Inorg. Chem.* **2002**, *41*, 590.
(42) Hitchcock, P. B.; Smith, J. D.; Thomas, K. M. *J. Chem. Soc., Dalton Trans.* **1976**, 1433.
(43) Harlan, C. J.; Mason, M. R.; Barron, A. R. *Organometallics* **1994**, *13*, 2957.

Chart 1

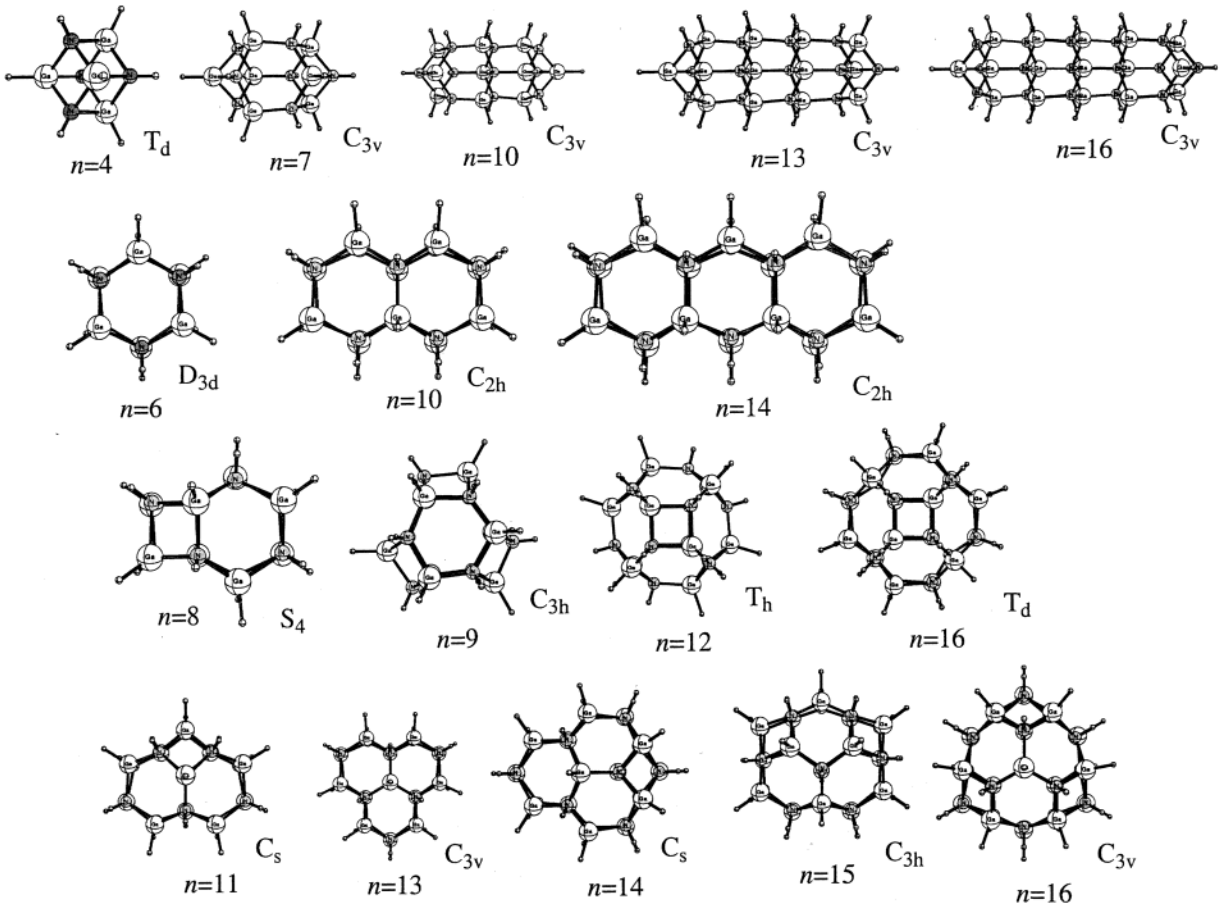

energy surfaces (PES) were characterized by the evaluation of analytic second derivatives and correspond to minima on the PES. The hybrid three-parameter exchange functional of Becke[44] with the gradient-corrected correlation functional of Lee, Yang, and Parr[45] (B3LYP) was used for the DFT studies. The polarized valence double-ζ (pVDZ) basis set of Ahlrichs and co-workers[46] was used for H (4s1p/2s1p), N (7s4p1d/3s2p1d), C (7s4p1d/3s2p1d), and Ga (14s10p5d/5s4p3d). The performance of the gallium effective core potential (ECP) basis set of Hay and Wadt,[47] augmented by d and p polarization functions, LANL2DZ-(d,p), was also tested. Orbital exponents were as follows: p exponent for H (1.0), and d exponents for N (0.8), C (0.75), and Ga (0.16). All computations were performed using the Gaussian 94[48] and Gaussian 98[49] program packages.

To obtain a reliable enthalpy of formation of gaseous GaH_3, which is not available experimentally, high-level ab initio computations [CCSD(T)[50] method with the cc-pVTZ basis set[51]] using the MOLPRO package[52] have been performed, resulting in the standard formation enthalpy for GaH_3(g) of 113.4 kJ mol^{-1}. Details on these computations may be found in the Supporting Information section.

Results and Discussion

I. Imidogallanes. A. Structural Features and Relative Energies. Only structures which possess gallium and nitrogen with coordination number 4 will be considered in the present work. It has been shown[29−32] that structures with coordination number 3 have a high tendency to dimerize to form nitrogen and aluminum/gallium centers, with most favorable coordination number 4. Oligomers with $n = 1-4, 6$ have been considered elsewhere[30] and will not be discussed here. In a schematic way, the structures of all considered oligomers are presented in Chart 1, while individual figures are provided as Supporting Information.

(44) Becke, A. D. *J. Chem. Phys.* **1993**, *98*, 5648.
(45) Lee, C.; Yang, W.; Parr, R. G. *Phys. Rev. B* **1988**, *37*, 785.
(46) Schafer, A.; Horn, H.; Ahlrichs, R. *J. Chem. Phys.* **1992**, *97*, 2571.
(47) (a) Hay, P. J.; Wadt, W. R. *J. Chem. Phys.* **1985**, *82*, 270. (b) Wadt, W. R.; Hay, P. J. *J. Chem. Phys.* **1985**, *82*, 284. (c) Hay, P. J.; Wadt, W. R. *J. Chem. Phys.* **1985**, *82*, 299.
(48) Frisch, M. J.; Trucks, G. W.; Schlegel, H. B.; Gill, P. M. W.; Johnson, B. G.; Robb, M. A.; Cheeseman, J. R.; Keith, T.; Petersson, G. A.; Montgomery, J. A.; Raghavachari, K.; Al-Laham, M. A.; Zakrzewski, V. G.; Ortiz, J. V.; Foresman, J. B.; Cioslowski, J.; Stefanov, B. B.; Nanayakkara, A.; Challacombe, M.; Peng, C. Y.; Ayala, P. Y.; Chen, W.; Wong, M. W.; Andres, J. L.; Replogle, E. S.; Gomperts, R.; Martin, R. L.; Fox, D. J.; Binkley, J. S.; Defrees, D. J.; Baker, J.; Stewart, J. P.; Head-Gordon, M.; Gonzalez, C.; Pople, J. A. *GAUSSIAN 94*, Revision C.3; Gaussian, Inc.: Pittsburgh, PA, 1995.
(49) Frisch, M. J.; Trucks, G. W.; Schlegel, H. B.; Scuseria, G. E.; Robb, M. A.; Cheeseman, J. R.; Zakrzewski, V. G.; Montgomery, J. A.; Stratmann, R. E.; Burant, J. C.; Dapprich, S.; Millam, J. M.; Daniels, A. D.; Kudin, K. N.; Strain, M. C.; Farkas, O.; Tomasi, J.; Barone, V.; Cossi, M.; Cammi, R.; Mennucci, B.; Pomelli, C.; Adamo, C.; Clifford, S.; Ochterski, J.; Petersson, G. A.; Ayala, P. Y.; Cui, Q.; Morokuma, K.; Malick, D. K.; Rabuck, A. D.; Raghavachari, K.; Foresman, J. B.; Cioslowski, J.; Ortiz, J. V.; Stefanov, B. B.; Liu, G.; Liashenko, A.; Piskorz, P.; Komaromi, I.; Gomperts, R.; Martin, R. L.; Fox, D. J.; Keith, T.; Al-Laham, M. A.; Peng, C. Y.; Nanayakkara, A.; Gonzalez, C.; Challacombe, M.; Gill, P. M. W.; Johnson, B.; Chen, W.; Wong, M. W.; Andres, J. L.; Gonzalez, C.; Head-Gordon, M.; Replogle, E. S.; Pople, J. A. *Gaussian 98*, Revision A.3; Gaussian, Inc.: Pittsburgh, PA, 1998.
(50) (a) Hampel, C.; Peterson, K.; Werner, H.-J. *Chem. Phys. Lett.* **1992**, *190*, 1. (b) Deegan, M. J. O.; Knowles, P. J. *Chem. Phys. Lett.* **1994**, *227*, 321.
(51) (a) Dunning, T. H. *J. Chem. Phys.* **1989**, *90*, 1007. (b) Woon, D. E.; Dunning, T. H. *J. Chem. Phys.* **1993**, *98*, 1358.
(52) Amos, R. D.; Bernhardsson, A.; Berning, A.; Celani, P.; Cooper, D. L.; Deegan, M. J. O.; Dobbyn, A. J.; Eckert, F.; Hampel, C.; Hetzer, G.; Knowles, P. J.; Korona, T.; Lindh, R.; Lloyd, A. W.; McNicholas, S. J.; Manby, F. R.; Meyer, W.; Mura, M. E.; Nicklass, A.; Palmieri, P.; Pitzer, R.; Rauhut, G.; Schütz, M.; Schumann, U.; Stoll, H.; Stone, A. J.; Tarroni, R.; Thorsteinsson, T.; Werner, H.-J. MOLPRO, a package of ab initio programs designed by H.-J. Werner and P. J. Knowles, Version 2002.1.

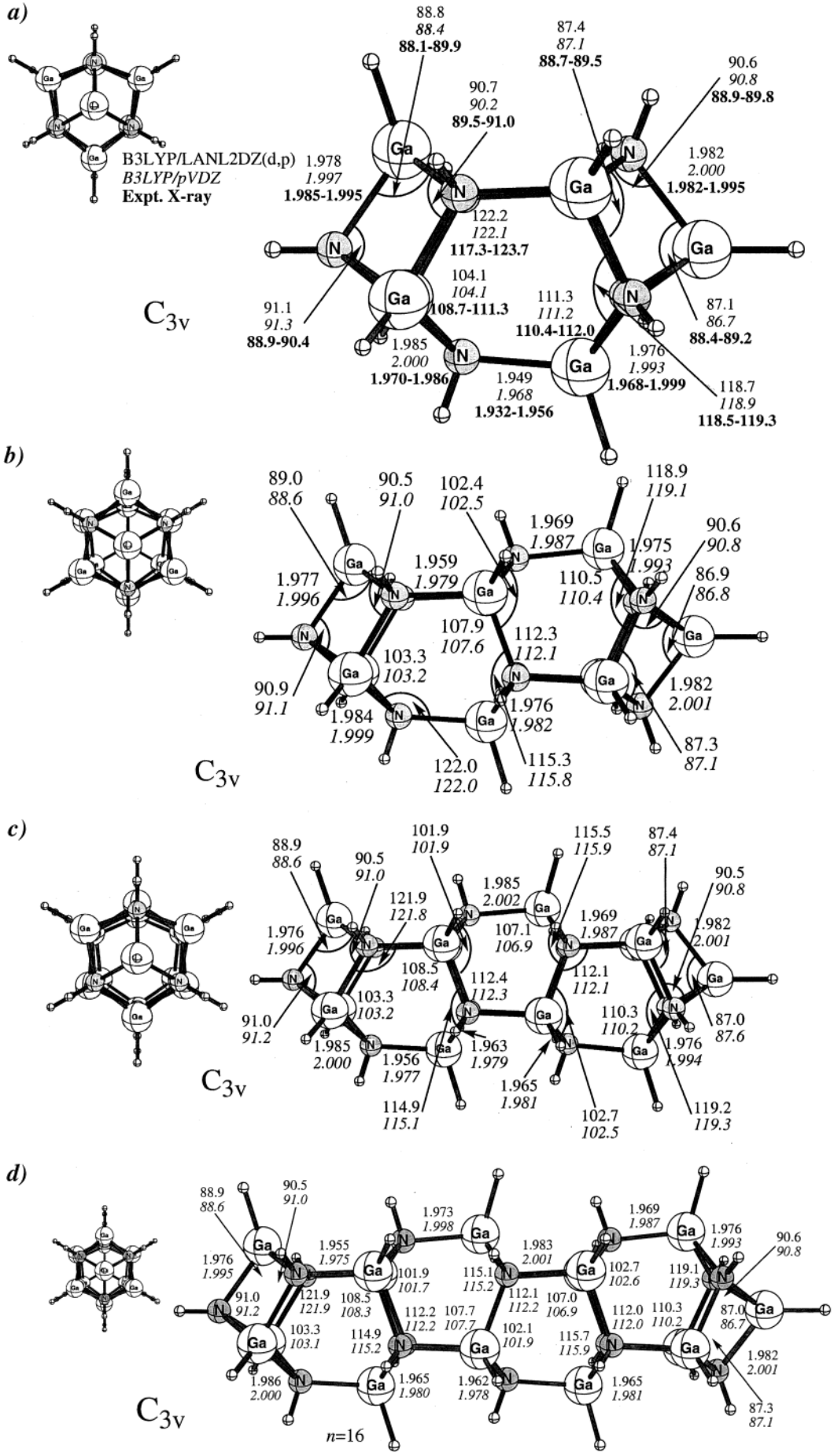
a)
B3LYP/LANL2DZ(d,p)
B3LYP/pVDZ
Expt. X-ray
1.978
1.997
1.985-1.995
88.8
88.4
88.1-89.9
87.4
87.1
88.7-89.5
90.6
90.8
88.9-89.8
90.7
90.2
89.5-91.0
1.982
2.000
1.982-1.995
122.2
122.1
117.3-123.7
104.1
104.1
108.7-111.3
111.3
111.2
110.4-112.0
91.1
91.3
88.9-90.4
87.1
86.7
88.4-89.2
1.985
2.000
1.970-1.986
1.976
1.993
1.968-1.999
1.949
1.968
1.932-1.956
118.7
118.9
118.5-119.3
C3v
b)
89.0
88.6
90.5
91.0
102.4
102.5
118.9
119.1
1.969
1.987
1.975
1.993
90.6
90.8
1.977
1.996
1.959
1.979
110.5
110.4
86.9
86.8
107.9
107.6
112.3
112.1
103.3
103.2
90.9
91.1
1.984
1.999
1.976
1.982
1.982
2.001
122.0
122.0
115.3
115.8
87.3
87.1
C3v
c)
88.9
88.6
90.5
91.0
101.9
101.9
115.5
115.9
87.4
87.1
90.5
90.8
1.985
2.002
121.9
121.8
1.969
1.987
1.982
2.001
1.976
1.996
107.1
106.9
108.5
108.4
112.4
112.3
112.1
112.1
103.3
103.2
91.0
91.2
110.3
110.2
87.0
87.6
1.985
2.000
1.956
1.977
1.963
1.979
1.976
1.994
1.965
1.981
114.9
115.1
102.7
102.5
119.2
119.3
C3v
d)
88.9
88.6
90.5
91.0
1.973
1.998
1.969
1.987
1.976
1.993
90.6
90.8
1.955
1.975
1.983
2.001
1.976
1.995
101.9
101.7
115.1
115.2
102.7
102.6
119.1
119.3
91.0
91.2
121.9
121.9
108.5
108.3
112.1
112.2
107.0
106.9
112.2
112.2
107.7
107.7
112.0
112.0
110.3
110.2
87.0
86.7
103.3
103.1
114.9
115.2
102.1
101.9
115.7
115.9
1.982
2.001
1.986
2.000
1.965
1.980
1.962
1.978
1.965
1.981
87.3
87.1
C3v
n=16

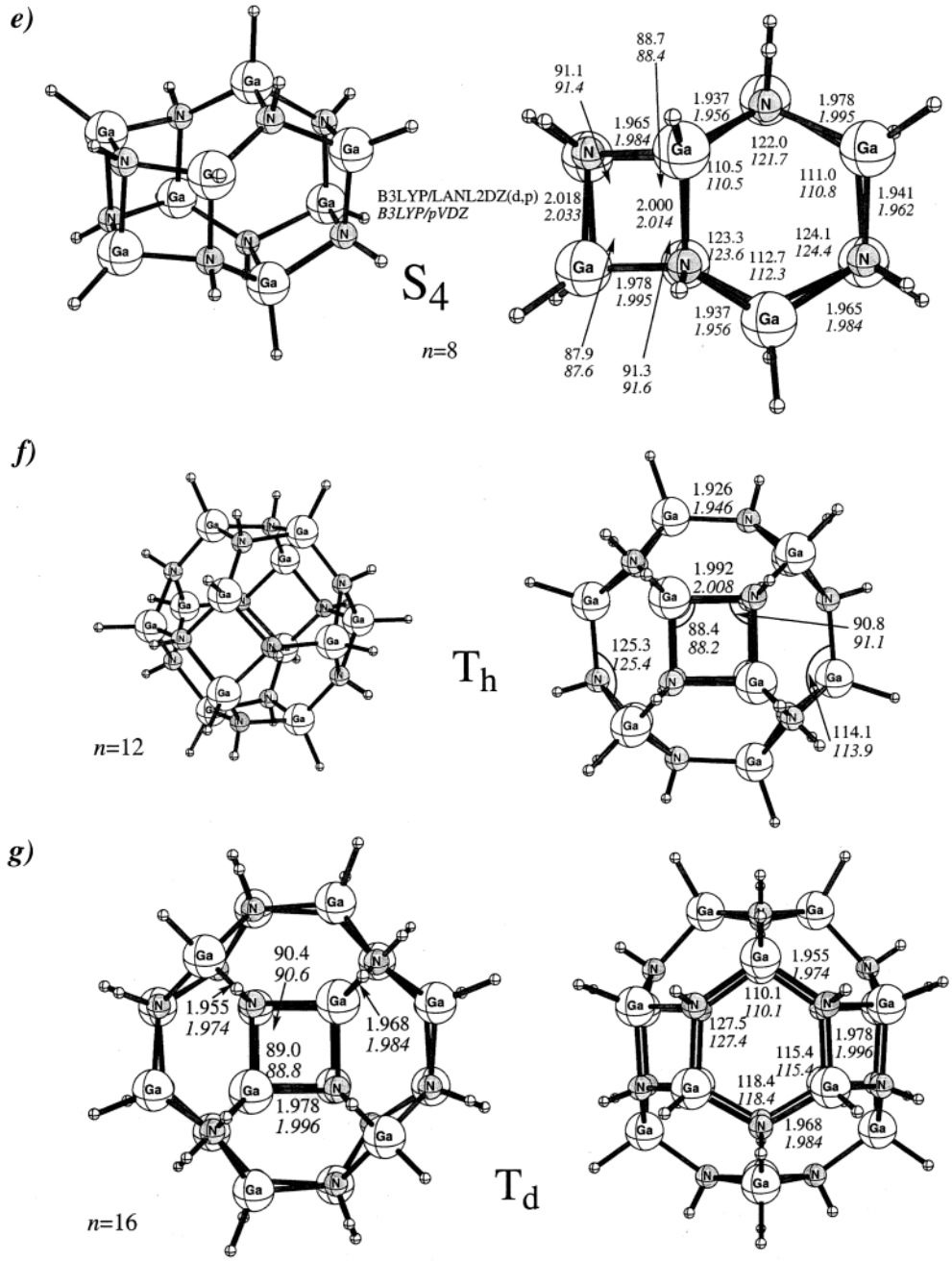

Figure 1. Structural parameters for selected imido compounds $[HGaNH]_n$. All distances are in angstroms, all angles in degrees.

Optimized structural parameters for the most important imidogallanes $[HGaNH]_n$ are given in Figure 1. Recently, the crystal structure of $[PhGaNMe]_7$ has been reported.[41] Comparison of our predicted Ga−N distances and bond angles (Figure 1a) shows good agreement with the experimental data. Ga−N bond distances predicted with the ECP basis set are generally shorter by 0.018 Å compared to those obtained with an all-electron basis set.

Relative energies for the several considered isomers (n = 10, 13, 14, 16) are summarized in Table 1. Comparison shows that, with increasing oligomerization degree n, needle-shaped structures become more stable compared to cages. While the difference between needle-shaped and cage (C_{2h} symmetric) isomers of $[HGaNH]_{10}$ is less than 4 kJ mol^{-1}, for $n = 13$ this difference is about 80 kJ mol^{-1} in favor of needle-shaped structure, and for $n = 16$ the difference is 98 and 123 kJ mol^{-1} (ECP and pVDZ basis sets, respectively) in favor of the needle-shaped isomer. High-mass needle-shaped oligomers were ignored in an earlier detailed computational study of methylaluminumoxanes[41] because the authors assumed that the presence of greater numbers of strained bonds (atoms in 3S and 2S + H environments) will lead to relative instability for such isomers. In stark contrast with these expectations, we found that, with the increase of n, it is the needle-shaped structures which turn out to be the most stable! We expect that this result may be generalizable to the isoelectronic clusters of the main group elements.

The higher stability of needle-shaped isomers with large oligomerization degrees may be rationalized in terms of the higher probability of structural relaxation. To form a stable closed cage, a good "match" between M−N bond distances and bond angles is needed. Closure of cage structure imposes strain

Table 1. Predicted Relative Energies E^{rel}, kJ mol^{-1}, for Several Isomers of the Considered Imidogallanes: B3LYP/pVDZ and (in parentheses) B3LYP/LANL2DZ(d,p) Levels of Theory

n	isomer	3S, 2S+H, 2H +S, 3H [a]	E^{rel}
10	$[HGaNH]_{10}$ (C_{3v} needle-shaped)	2, 6, 6, 6	0.0 (0.0)
	$[HGaNH]_{10}$ (C_{2h} cage)	0, 8, 8, 4	3.7 (−0.2)
13	$[HGaNH]_{13}$ (C_{3v} needle-shaped)	2, 6, 6, 12	0.0 (0.0)
	$[HGaNH]_{13}$ (C_{3v} cage)	0, 6, 12, 8	81.8 (75.6)
14	$[HGaNH]_{14}$ (C_{2h} cage)	0, 8, 8, 12	0.0 (0.0)
	$[HGaNH]_{14}$ (C_s cage)	0, 2, 20, 6	40.8 (29.9)
16	$[HGaNH]_{16}$ (C_{3v} needle-shaped)	2, 6, 6, 18	0.0 (0.0)
	$[HGaNH]_{16}$ (T_d cage)	0, 0, 24, 8	122.8 (97.9)
	$[HGaNH]_{16}$ (C_{3v} cage)	0, 0, 24, 8	134.0 (111.3)

[a] 3S, 2S+H, 2H+S, and 3H are the number of atoms in corresponding positions (3S means sharing three square faces; 2S+H means sharing two square and one hexagonal; etc).

upon all the atoms in the structure. In contrast, for the needle-shaped structures, only atoms situated in the "capping" region are highly strained, but atoms in the middle Ga_3N_3 rings (3H positions) are very well suited for "relaxation". As the number of such "relaxed" atoms increases with the oligomerization degree, the stability of the needle structures increases with *n*. This conclusion is supported by both energetic and structural arguments. Table 2 presents subsequent oligomerization enthalpies for the needle-shaped clusters. Subsequent oligomerization enthalpies are exothermic, but decrease in absolute value with increasing *n*, indicating the achievement of "saturation" for the structure. A similar pattern is observed for the mean Ga−N distance in the clusters, which decreases from 2.001 Å in $[HGaNH]_4$ to 1.989 Å in $[HGaNH]_{16}$.

In further discussions here, connected with the thermodynamics of imidogallanes, for the each oligomerization degree *n*, only one (the most stable) isomer will be taken for the evaluation of the thermodynamic properties.

B. Energetics of the Oligomerization Reactions. Figure 2 presents trends in changes of the standard enthalpy, entropy, and Gibbs energy for the reaction 1 as a function of the oligomerization degree *n*.

$$[HGaNH] \rightarrow {}^1/_n[HGaNH]_n \qquad (1)$$

Results for the entropy change obtained with full electron and ECP basis sets are almost identical. Negative (unfavorable) reaction entropies rapidly decrease for small *n*. The entropy change per mole of monomer becomes consistent after $n = 9$, and for the last eight members of oligomer series ($n = 9-16$) it may be approximated by the following equations (values in J mol^{-1} K^{-1}):

B3LYP/pVDZ: $\Delta S^0_{298}(1) = -1.4181n - 163.4$, correlation coefficient 0.985

B3LYP/LANL2DZ(d,p): $\Delta S^0_{298}(1) = -1.4072n - 163.8$, correlation coefficient 0.980.

It is expected that this linear trend in oligomerization entropy may be extrapolated for the oligomers with higher oligomerization degrees ($n > 16$).

Standard enthalpies for process (1) are negative (favorable) for all *n*. With the increase of the oligomerization degree up to 6, the oligomerization enthalpy increases significantly. Thereafter, changes are less pronounced but have a complicated

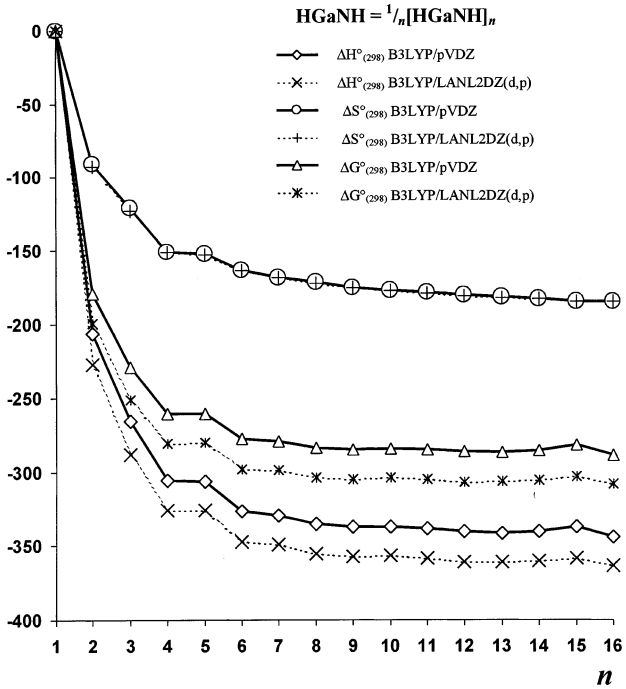

Figure 2. Trends of the standard enthalpy, entropy, and Gibbs energy for the reaction $[HGaNH] \rightarrow {}^1/_n[HGaNH]_n$ as a function of the oligomerization degree *n*. Abscissa: oligomerization degree *n*. Ordinate: standard enthalpies $\Delta H^0_{298}(1)$ and standard Gibbs energies $\Delta G^0_{298}(1)$ are in kJ mol^{-1}; standard entropies $\Delta S^0_{298}(1)$ are in J mol^{-1} K^{-1}.

Table 2. Subsequent Oligomerization Enthalpies (kJ mol^{-1}) of Needle-Shaped Clusters: ${}^1/_n[HGaNH]_n \rightarrow {}^1/_{(n+3)}[HGaNH]_{(n+3)}$ per Mole of Monomer

	B3LYP/LANL2DZ(d,p)		B3LYP/pVDZ	
process	ΔH^0_{298}	ΔS^0_{298}	ΔH^0_{298}	ΔS^0_{298}
${}^1/_4[HGaNH]_4 \rightarrow {}^1/_7[HGaNH]_7$	−22.5	−17.8	−22.5	−17.3
${}^1/_7[HGaNH]_7 \rightarrow {}^1/_{10}[HGaNH]_{10}$	−7.3	−8.5	−7.4	−8.5
${}^1/_{10}[HGaNH]_{10} \rightarrow {}^1/_{13}[HGaNH]_{13}$	−4.2	−4.7	−4.2	−4.7
${}^1/_{13}[HGaNH]_{13} \rightarrow {}^1/_{16}[HGaNH]_{16}$	−2.6	−3.0	−2.7	−3.2

pattern. Results obtained with both ECP and all-electron basis sets exhibit a similar general trend, but absolute values of standard enthalpies predicted at the B3LYP/LANL2DZ(d,p) level of theory are by 18.8−22.0 (on average 19.6) kJ mol^{-1} lower (more negative) compared to those obtained at the B3LYP/pVDZ level. Changes in the standard Gibbs energies follow the trend observed for the enthalpies. It is remarkable that $\Delta G^0_{298}(1)$ is the most negative for $n = 16$ at both B3LYP/pVDZ and B3LYP/LANL2DZ(d,p). This finding makes the needle-shaped cluster (Figure 1d) exceptionally stable at low temperatures.

Figure 3 presents trends in relative abundances of different clusters with increasing temperature. These abundances have been calculated in the manner described in ref 40, on the assumption of an equilibrium between all the imido compounds in the gas phase. Note that the needle-shaped cluster with $n = 16$ dominates the gas phase up to 600−650 K. As the temperature increases further, low-mass clusters became more pronounced due to the entropy factor. At the B3LYP/LANL2DZ(d,p) level of theory, the cage structure $[HGaNH]_{12}$ has considerable abundance, with maximum concentration at about 500 K. The octamer and hexamer have considerable abundances at temperatures higher than 600 K. Finally, only at very high temperatures is the existence of trimeric imido compounds

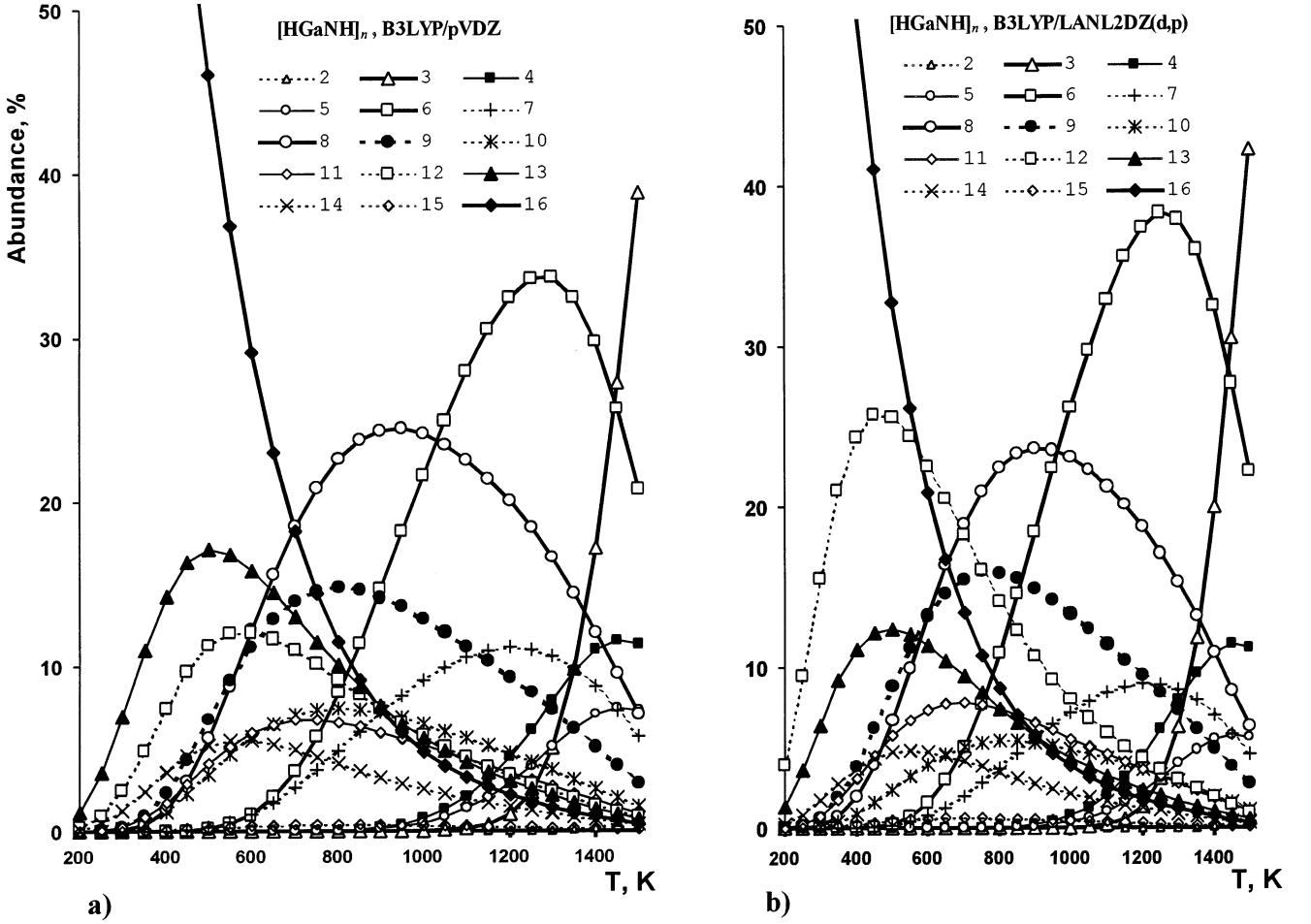

Figure 3. Relative abundances (%) of the $[HGaNH]_n$ clusters as a function of temperature. (a) B3LYP/pVDZ and (b) B3LYP/LANL2DZ(d,p) level of theory.

possible thermodynamically. Figure 4 gives a graphical representation of the abundances vs oligomerization degree at 500, 1000, and 1500 K.

The assumption about the equilibrium between different oligomers is partly supported by available experimental evidence. For example, the formation of several $[EtGaNEt]_n$ compounds was observed in recent laboratory work,[53] from which $[EtGaNEt]_6$ has been extracted at 115 °C in toluene solution, which "indicated an effective conversion of other clusters in the family of $[EtGaNEt]_n$ to $[EtGaNEt]_6$". Reversible interconversions of different isomers have been observed for analogous $[tBuGaS]_n$[54] and alkylaluminum oxide $[RAlO]_n$ clusters.[40,55,56] On the other hand, $[MeAlNMe]_7$ and $[MeAlNMe]_8$ interconvert only slowly in toluene solution at ca. 200 °C, although it was possible to separate the two by vacuum sublimation at 10^{-3} Torr.[57] Due to the higher Al−N bond strength, the activation barrier for interconversion may be significantly higher for imidoalanes than for the $[tBuGaS]_n$ clusters.[54] Since the Ga−N bond in clusters is significantly weaker compared to the Al−N bond,[31] the rearrangement of imidogallanes may proceed much more easily compared to that of imidoalanes.

C. Thermodynamics of Cluster Formation from GaH_3 and NH_3. Reaction to yield cluster formation from gaseous GaH_3 and NH_3 molecules (process (2)) may been considered. Enthalpies and entropies of oligomerization, evaluated per mole of monomer, are summarized in Table 4. Figure 5 presents the Gibbs energies calculated for reaction 2 at 298, 500, 750, and 1000 K. Predictions obtained at the B3LYP/pVDZ level of theory are given, and results obtained at the B3LYP/LANL2DZ-(d,p) level are qualitatively similar. The Gibbs energies for process (2) become negative (favorable) starting from $n = 2$. The exothermicity significantly increases with the increase of n to 6, while further changes are less pronounced. Note that as the temperature increases, the Gibbs energies became less negative due to the unfavorable entropy contributions. However, even at 1000 K the values of the Gibbs energy for high oligomers are below -50 kJ mol^{-1}, indicating the high favorability of their formation from GaH_3 and ammonia. Thus, we conclude that reaction between GaH_3 and ammonia should produce clusters with high oligomerization degrees in a broad temperature range.

$$GaH_3 + NH_3 \rightarrow {}^1/_n[HGaNH]_n + 2H_2 \qquad (2)$$

(53) Luo, B.; Gladfelter, W. L. *J. Cluster Sci.* **2002**, *13*, 461.
(54) Power, M. B.; Ziller, J. W.; Barron, A. R. *Organometallics* **1992**, *11*, 2783.
(55) Pasynkiewicz, S. *Polyhedron* **1990**, *9*, 429.
(56) Mason, M. R.; Smith, J. M.; Bott, S. G.; Barron, A. R. *J. Am. Chem. Soc.* **1993**, *115*, 4971.
(57) Amirkhalili, S.; Hitchcock, P. B.; Smith, J. D. *J. Chem. Soc., Dalton Trans.* **1979**, 1206.

Table 3. Mean Ga−N Bond Distances r(Ga−N) in Angstroms and Dipole Moments μ in Debye, for Amido-imido Gallanes and Related Needle-Shaped Imido Gallanes[a]

$[H_2GaNH_2]_3[HGaNH]_{3m}$			$[HGaNH]_n$				ΔH^0_{298}	ΔS^0_{298}
m	r(Ga–N)	μ	n	r(Ga–N)	μ	Δr(Ga–N)	capping	capping
0	2.0287	1.39	4	2.0010	0	0.0277	−13.3	192.1
1	2.0026	8.28	7	1.9930	1.56	0.0096	−79.1	229.1
2	1.9955	14.19	10	1.9911	2.56	0.0044	−109.7	232.3
3	1.9922	21.18	13	1.9901	3.76	0.0021	−136.6	230.4

[a] Shrinkage of mean Ga−N bond upon capping Δr(Ga−N), and thermodynamic characteristics for the capping reactions $[H_2GaNH_2]_3[HGaNH]_{3m} + GaH_3 + NH_3 \rightarrow [HGaNH]_n + 5H_2$. Standard enthalpies ΔH^0_{298} are in kJ mol^{-1}, standard entropies ΔS^0_{298} in J mol^{-1} K^{-1}. B3LYP/pVDZ level of theory.

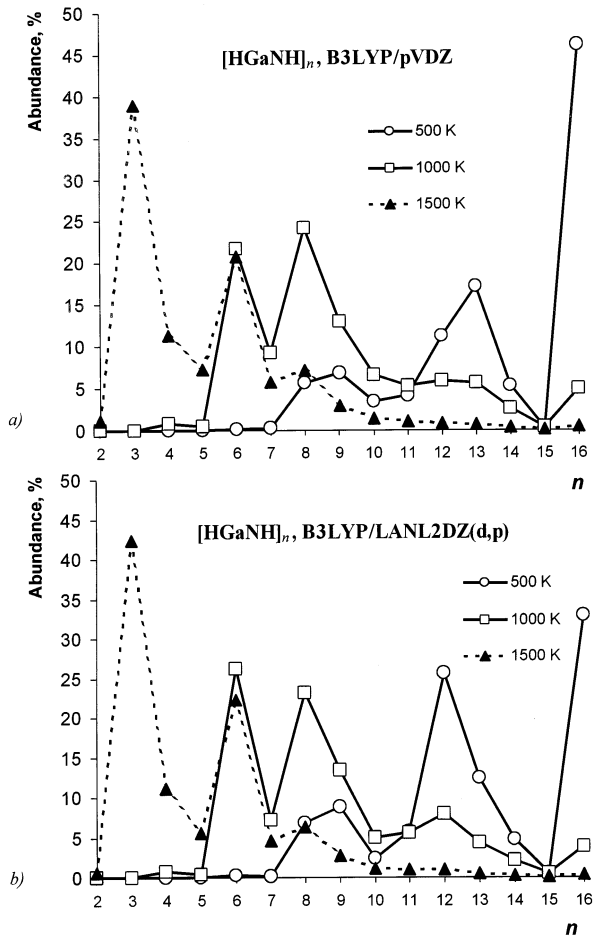

Figure 4. Trends in isomer abundances at different temperatures as a function of oligomerization degree n.

The effect of the pressure P on the thermodynamics of cluster formation from GaH_3 and ammonia will be briefly discussed. Considering reaction 2, one notes that it has an increasing number of the gaseous moles (by $1/n$); therefore, *decreasing* pressure should favor cluster formation from GaH_3 and NH_3. However, due to the fact that the number of gaseous moles evolved is decreasing with increasing n, in practice changes of the pressure lead to very minor changes of the Gibbs energy for the clusters with high oligomerization degrees n. Thus, at standard temperature 298 K, changing the pressure by up to 4 orders of magnitude (from 1 to 10^{-4} atm) results in decreasing the Gibbs energy by less than 2 kJ mol^{-1} for $n \geq 12$. At 1000 K, the change of the Gibbs energy is about 3 times larger (less than 6 kJ mol^{-1} for $n \geq 12$). Therefore, we conclude that reactor pressure has only a minor effect on the thermodynamics of process (2) for large clusters. Despite the fact that pressure should be *decreased* to make formation of imidogallanes slightly more favorable thermodynamically, in practical work it would be better to employ *higher* pressure conditions (which are only

Table 4. Thermodynamic Characteristics of the Reaction $GaH_3 + NH_3 \rightarrow {}^1/_n [HGaNH]_n + 2H_2$[a]

	B3LYP/LANL2DZ(d,p)		B3LYP/pVDZ	
n	ΔH^0_{298}	ΔS^0_{298}	ΔH^0_{298}	ΔS^0_{298}
1	185.9	101.2	189.3	101.5
2	−41.7	8.2	−17.5	10.5
3	−102.3	−21.9	−76.0	−19.9
4	−139.8	−50.2	−116.8	−50.2
5	−140.0	−52.0	−116.9	−51.3
6	−161.1	−62.7	−137.1	−62.2
7	−163.2	−68.0	−140.2	−67.4
8	−169.5	−71.5	−145.9	−70.7
9	−171.6	−74.8	−147.9	−74.3
10	−170.8	−76.3	−147.9	−76.0
11	−172.7	−78.1	−148.9	−77.5
12	−175.5	−80.0	−151.1	−79.5
13	−175.2	−81.3	−152.2	−80.7
14	−174.5	−82.3	−151.2	−81.7
15	−172.6	−84.3	−148.1	−83.6
16	−177.9	−84.3	−155.1	−83.9

[a] Standard enthalpies ΔH^0_{298} are in kJ mol^{-1}, standard entropies ΔS^0_{298} in J mol^{-1} K^{-1}.

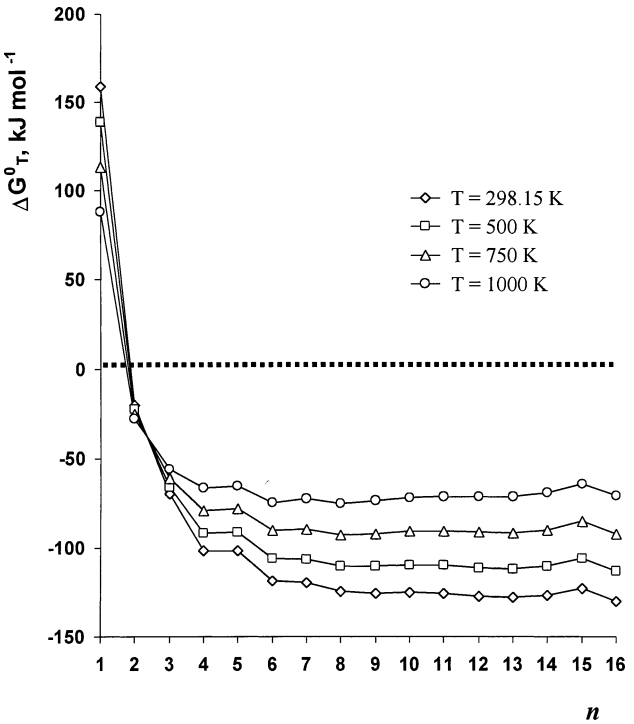

Figure 5. Toward the estimation of the highest oligomerization degree. Gibbs energy of the reaction $GaH_3 + NH_3 \rightarrow {}^1/_n[HGaNH]_n + 2H_2$ as a function of oligomerization degree n at several temperatures. B3LYP/pVDZ level of theory.

Table 5. Estimated Highest Oligomerization Degree *n* for Which the Reaction of Oligomer Formation Is Thermodynamically Favorable (at Different Temperatures)

	B3LYP/LANL2DZ(d,p)				B3LYP/pVDZ			
reaction	298 K	500 K	750 K	1000 K	298 K	500 K	750 K	1000 K
$GaH_3 + NH_3 \rightarrow {}^1/_n\,[HGaNH]_n + 2H_2$	462	252	149	97	387	208	120	76
${}^1/_3[H_2GaNH_2]_3 \rightarrow {}^1/_n\,[HGaNH]_n + H_2$	113	90	79	73	66	62	60	59

slightly thermodynamically disfavorable) to perform better kinetically.

D. Estimation of the Highest Oligomerization Degree of Gas-Phase Clusters. What is the maximal size of the oligomers which can be formed in the gas phase? Obviously, entropy factors disfavor cluster formation. However, as may be seen from Figure 5, the entropy factor is fully compensated by the highly negative enthalpies of formation. Therefore, formation of clusters with $n > 16$ should be viable. To estimate the highest oligomerization degree for which formation of clusters will be thermodynamically favorable, we focus on the most stable needle-shaped structures, those with $n = 4$, 7, 10, 13, and 16. Subsequent enthalpies and entropies of oligomerization, evaluated per mole of monomer, are summarized in Table 2. Note that the subsequent oligomerization enthalpy is favorable up to $n = 16$. Upon growth of the cluster, changes in subsequent enthalpies become less pronounced. This observation fits together with the "saturation model" (changes in the mean Ga−N distance in the 4, 7, 10, 13 series become less and less pronounced in Table 3). One may assume that, for the larger members of the needle-shaped family, subsequent oligomerization enthalpies will become zero. Therefore, approximating the enthalpy of the larger clusters with the value obtained for the highest oligomer ($n = 16$) and taking into account the fact that the entropy change disfavors the cluster formation (see equations in section IB above), one may estimate the value of the oligomerization degree *n*, at which the Gibbs energy of the reaction 2 will be equal to zero. These highest thermodynamically favored oligomerization degrees depend on the temperature, and predicted values for several temperatures are given in Table 5. In the same manner, the highest oligomerization degrees from the cyclotrigallazane (process ${}^1/_3[H_2GaNH_2]_3 \rightarrow {}^1/_n[HGaNH]_n + H_2$) have also been estimated. At room temperature the results are 66 and 113 for the pVDZ and LANL2DZ(d,p) basis sets, respectively, and decrease with increasing temperature. All predictions (Table 5) indicate that a spontaneous generation of needle-shaped clusters with *n* of at least 60 is thermodynamically favorable in a broad temperature range, using either GaH_3 and ammonia or cyclotrigallazane as source compounds.

II. Amido-imido Compounds. A. "Open Needles" and Their Capping. Since, as follows from this work, needle-shaped structures are expected to dominate the gas phase at low temperatures, they attracted our attention. The mechanistic pathway of their formation from the trimeric cyclotrigallazane is proposed. It includes dimerization (polymerization) of two or more $[H_2GaNH_2]_3$ rings with formation of amido-imido compounds, followed by their capping (Scheme 1). Therefore, we theoretically investigate several members of the series of amido-imido compounds of general formula $[H_2GaNH_2]_3$-$[HGaNH]_{3m}$. The first compound in this series ($m = 0$) is a trimeric amido compound, the well-known cyclotrigallazane itself.[58] Increasing the value of *m* leads to an increase of the "imide" character of the compound. For $m \rightarrow \infty$, the inorganic polymer rod terminated on both sides (on one side by amido groups and on the other side by GaH_2 groups) is obtained. In Figure 6, structures of the first three members of the series with $m = 1$, 2, and 3 are presented. Their capping will lead to needle-shaped oligomers with $n = 7$, 10, and 13, respectively (Figure 1a−c). The experimentally structurally characterized amido-imido gallane, $[MeGaNMe]_6[Me_2GaNHMe]_2$, has a different structural motif.[57] However, recent mass spectrometry data are consistent with the presence of $[Me_9M_6N_6H_9]$ clusters in vapors, for which a structure equivalent to the one in Figure 6a can be assumed.[27]

Table 3 presents structural and thermodynamic characteristics of the capped and uncapped "needles". With increasing oligomerization degree, the mean Ga−N distance decreases in both series, indicating structural relaxation. This factor significantly influences the relative stability of the needle-shaped isomers with respect to cages. Dipole moments also increase in both series. Especially intriguing are the structural and thermodynamic changes accompanying the capping process. Upon capping, the mean Ga−N bond length shortens. The most noticeable change of Ga−N distance is observed for capping cyclotrigallazane. Figure 7 presents the trends in capping enthalpies and shortening of the Ga−N bond. Capping enthalpies are always exothermic, and, surprisingly, the exothermicity of the capping process increases with the oligomerization degree (-13 kJ mol^{-1} for $m = 0$ to -137 kJ mol^{-1} for $m = 3$). Since entropy factors also favor the capping process, we conclude that amido-imido compounds may be viable intermediates in the generation of needle-shaped imido compounds.

We tentatively assume that formation of the amido-imido compounds proceeds by polymerization of cyclotrigallazane. To this end, thermodynamic parameters of the consecutive ring fusions (per mole of cyclotrigallazane) are presented in Table 6. Cyclotrigallazane can dimerize in two ways—with elimination of 6 mol of H_2 and formation of six new Ga−N bonds (resulting in hexamers $[HGaNH]_6$), or by dimerization with elimination of 3 mol of H_2, forming $[H_2GaNH_2]_3[HGaNH]_3$ (Scheme 1). The enthalpy of dimerization of cyclotrigallazane with formation of only three Ga−N bonds is endothermic, but is favored by entropy. This is contrary to the formation of hexamers structure with six Ga−N bonds formed, which is exothermic. Thus, dimerization of cyclotrigallazine with formation of the hexamer imido compound $[HGaNH]_6$ is more favorable (compared to $[H_2GaNH_2]_3[HGaNH]_3$) at all temperatures. Note that at room temperature, the Gibbs energy of formation of the higher amido-imido oligomers is more negative, compared to $[HGaNH]_6$. This makes the amido-imido oligomers suitable intermediates in conversion of cyclotrigallazane to polymeric imidogallanes. As

(58) Campbell, J. P.; Hwang, J. W.; Young, V. G.; Von Dreele, R. B.; Cramer, C. J.; Gladfelter, W. L. *J. Am. Chem. Soc.* **1998**, *120*, 521.

Scheme 1

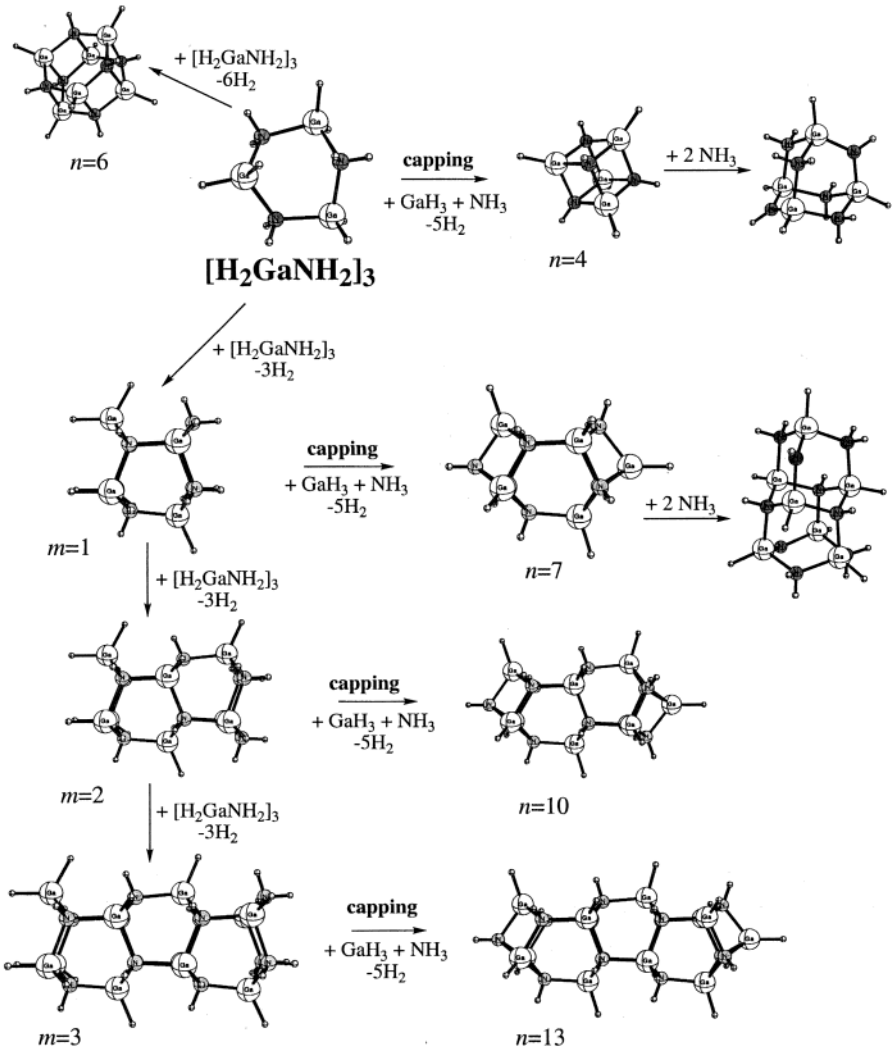

may be seen (Table 6), formation of $[HGaNH]_{16}$ is the most favorable process at low temperatures.

B. Adamantane-Type Structures: Reactions of Imido Compounds with Ammonia. Under CVD conditions, an excess of ammonia is usually employed. Thus, it is of interest to study the reactivity of needle-shaped oligomers toward ammonia. Amido-imido clusters, which are potential intermediates of the production of imido compounds, have been structurally characterized by Luo and Gladfelter.[59] They have adamantane-like Ga_4N_6 and Ga_7N_9 cores. The simplest analogues of synthesized clusters have been considered (Scheme 1). The formulas for these compounds would be $[HGaNH]_4 \cdot NH_3$, $[HGaNH]_4 \cdot 2NH_3$, and $[HGaNH]_7 \cdot 2NH_3$. For the each compound two isomers, which differ by the orientation of the NH groups, are possible. Optimized structures of the most stable isomers are shown in Figure 8; alternative structures are higher in energy by 37.6, 43.8, and 14.7 kJ mol^{-1} for $Ga_4N_5H_{11}$, $Ga_4N_6H_{14}$, and $Ga_7N_9H_{20}$, respectively.

The processes of their formation,

$$[HGaNH]_4 + 2NH_3 \rightarrow Ga_4N_6H_{14}; \qquad [HGaNH]_7 + 2NH_3 \rightarrow Ga_7N_9H_{20} \quad (3)$$

from imido compounds and ammonia are thermodynamically favorable at low temperatures (Table 7). But as the temperature increases, entropy favors ammonia elimination. At 750 K, the Gibbs energies of the processes are positive. In accord with our predictions, experimentally synthesized adamantane-type species, on heating, were found by Luo and Gladfelter to be partly converted to the corresponding tetramer and heptamer units.[59] Such reactions once again point to a nonrigid structure for Ga−N-based oligomers. As the data in Table 7 indicate, the heptamer-based adamantane structure loses ammonia more easily, which can be explained by the greater stability of the heptamer compared to the tetramer cluster. From this point of view, for the larger oligomerization degrees, the excess ammonia will be eliminated more readily.

One may also discuss the formation of these compounds from GaH_3 and ammonia according to the following reactions:

$$GaH_3 + {}^3/_2NH_3 \rightarrow {}^1/_4[Ga_4N_6H_{14}] + 2H_2$$

$$GaH_3 + {}^9/_7NH_3 \rightarrow {}^1/_7[Ga_7N_9H_{20}] + 2H_2$$

These processes are favorable by enthalpy but disfavored by entropy. Comparison of the thermodynamic parameters in Tables

(59) Luo, B.; Gladfelter, W. L. *Inorg. Chem.* **2002**, *41*, 6949.

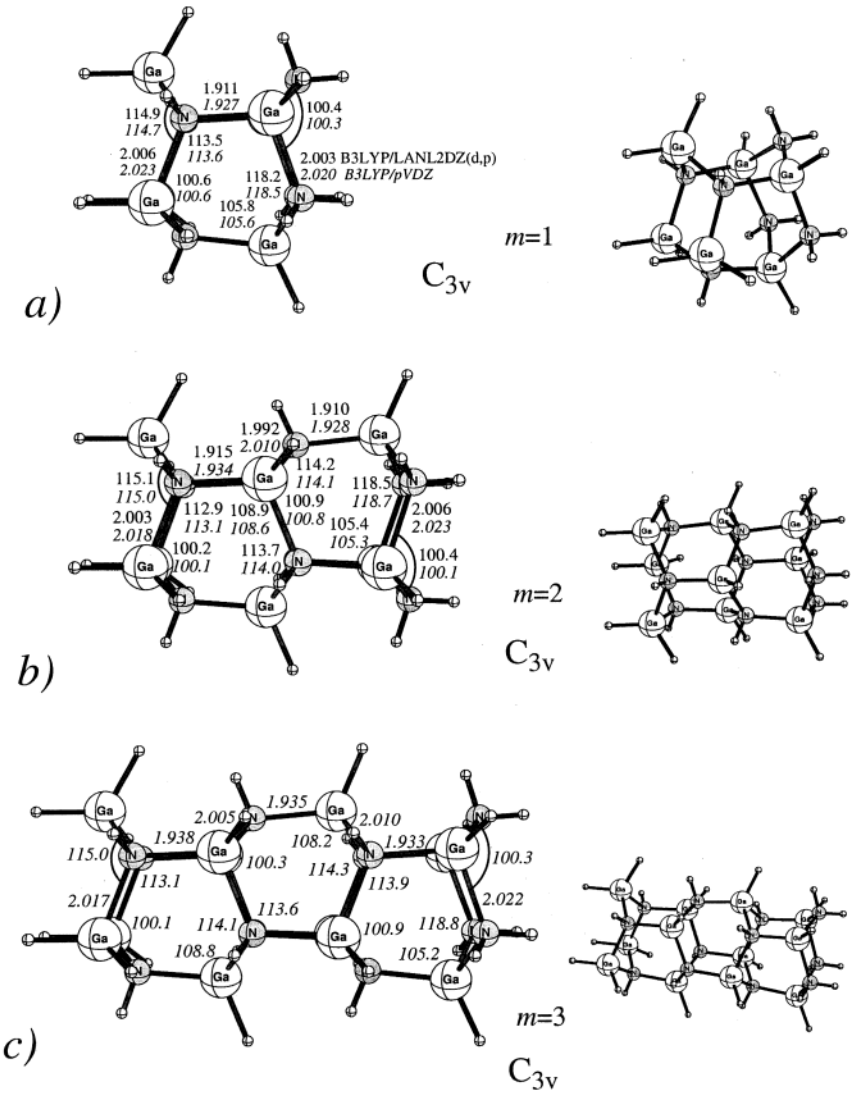

Figure 6. Optimized parameters of amido-imido $[H_2GaNH_2]_3[HGaNH]_{3m}$ compounds. All distances are in angstroms, all angles in degrees.

Table 6. Thermodynamic Characteristics for the Oligomerization of Cyclotrigallazane[a]

process	ΔH^0_{298}	ΔS^0_{298}	ΔG^0_{298}	ΔG^0_{500}	ΔG^0_{750}	ΔG^0_{1000}
$[H_2GaNH_2]_3 \rightarrow {}^1/_2\,[HGaNH]_6 + 3H_2$	42.7	206.2	−18.7	−60.4	−111.9	−163.5
$[H_2GaNH_2]_3 \rightarrow {}^1/_2\,[H_9Ga_6N_6H_9] + {}^3/_2H_2$	2.7	42.2	−9.8	−18.3	−28.9	−39.4
$[H_2GaNH_2]_3 \rightarrow {}^1/_3\,[H_{12}Ga_9N_9H_{12}] + 2H_2$	−2.5	62.0	−21.0	−33.5	−49.0	−64.5
$[H_2GaNH_2]_3 \rightarrow {}^1/_4\,[H_{15}Ga_{12}N_{12}H_{15}] + {}^9/_4H_2$	−6.7	73.0	−28.4	−43.1	−61.4	−79.6
$[H_2GaNH_2]_3 \rightarrow {}^3/_{16}\,[HGaNH]_{16} + 3H_2$	−11.3	141.1	−53.3	−81.8	−117.1	−152.4

[a] Standard enthalpies and Gibbs energies are in kJ mol^{-1}, standard entropies in J mol^{-1} K^{-1}. B3LYP/pVDZ level of theory.

Table 7. Thermodynamic Properties of the Reactions Leading to Adamantane-Type Structures[a]

process	ΔH^0_{298}	ΔS^0_{298}	ΔG^0_{298}	ΔG^0_{750}	$T_{K=1}$
$[HGaNH]_4 + NH_3 \rightarrow Ga_4N_5H_{11}$	−78.4	−113.9	−44.4	7.0	688
$[HGaNH]_4 + 2NH_3 \rightarrow Ga_4N_6H_{14}$	−187.4	−262.6	−109.1	9.6	714
$[HGaNH]_7 + 2NH_3 \rightarrow Ga_7N_9H_{20}$	−152.3	−269.9	−71.9	50.1	564
$GaH_3 + {}^5/_4NH_3 \rightarrow {}^1/_4[Ga_4N_5H_{11}] + 2H_2$	−136.4	−78.6	−112.9	−77.4	1735
$GaH_3 + {}^3/_2NH_3 \rightarrow {}^1/_4[Ga_4N_6H_{14}] + 2H_2$	−163.6	−115.8	−129.1	−76.8	1410
$GaH_3 + {}^9/_7NH_3 \rightarrow {}^1/_7[Ga_7N_9H_{20}] + 2H_2$	−162.0	−106.0	−130.4	−82.5	1530

[a] Standard enthalpies and Gibbs energies are in kJ mol^{-1}, standard entropies in J mol^{-1} K^{-1}. Temperatures at which the equilibrium constant equals one, $T_{K=1}$, in K. B3LYP/pVDZ level of theory.

4 and 7 indicates that, although the adamantane-type clusters are formed more exothermically, the entropy contribution is much less favorable. Therefore, their generation is expected to occur for CVD conditions at low temperatures, especially if an excess of ammonia is present. Upon heating, the adamantane-like clusters are expected to liberate extra ammonia and convert to needle-shaped imido compounds.

III. Thermodynamics of the GaN CVD Process. Gibbs Energy−Temperature Diagram. Figure 9 presents a Gibbs energy−temperature diagram for the most important reactions

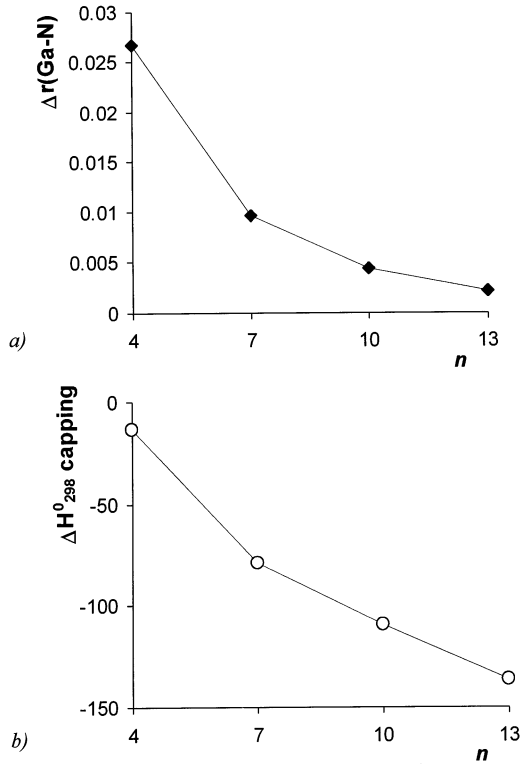

Figure 7. Trends in GaN bond shortening (a) and capping enthalpies (b).

starting from GaH_3 and NH_3. In addition to data predicted at the B3LYP/pVDZ level of theory, the experimental data for the formation of liquid Ga metal and solid gallium nitride GaN have been used.[60] The new experimental standard enthalpy of formation of GaN(s) (-156.8 ± 16 kJ mol^{-1}) has been used.[61] As for GaH_3(g), there are no experimental thermodynamic data available. Therefore, the formation enthalpy of GaH_3(g) has been predicted at the CCSD(T) level of theory, the resulting value being 113.4 kJ mol^{-1} (see Supporting Information for more details).

As may be seen, at low temperatures the most thermodynamically favorable product in the gas-phase reaction between gaseous GaH_3 and NH_3 is solid gallium nitride. Only at higher temperatures (about 1000 °C) does its dissociation with formation of a liquid Ga metal and N_2 take place. Among the *gas-phase* reactions, the imido compounds should dominate at low temperatures. As the temperature increases, higher oligomers become less stable due to entropy factors: in the temperature range 500−750 K several oligomers have similar abundances, and at temperatures higher than 825 K, the hexamer compound $[HGaNH]_6$ is predicted to become the most stable gas-phase molecule. Its stability lasts until 920 K, when reactions with formation of the small molecules GaH, N_2, and H_2 become dominant due to entropy factors.

From the diagram, gaseous imido compounds with high oligomerization degrees can be important intermediates in the growth of GaN. Their gas-phase generation is very favorable thermodynamically, and these oligomers may serve as a basis

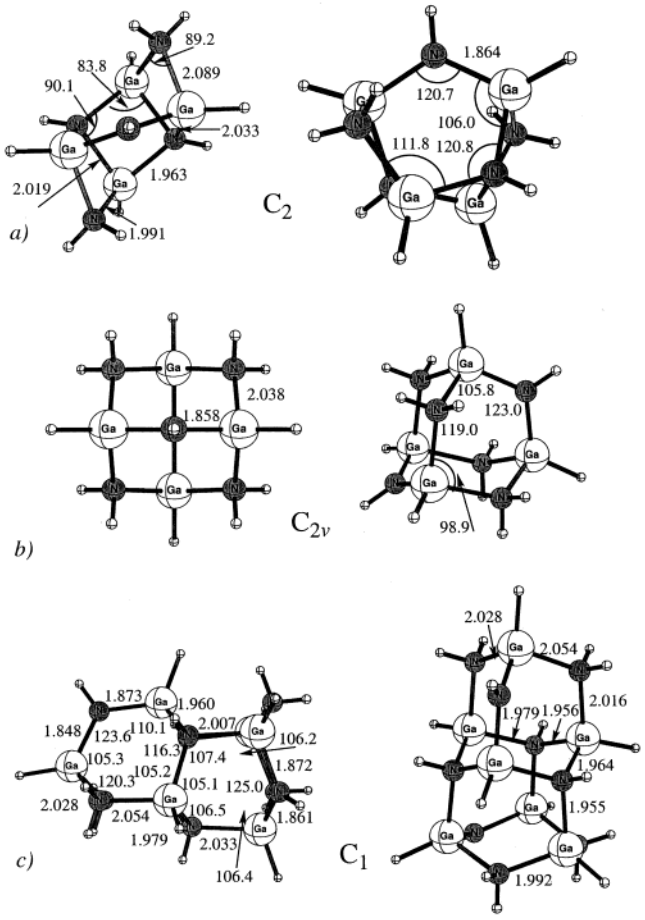

Figure 8. Optimized parameters of the most stable adamantane-type structures: (a) $[HGaNH]_4 \cdot NH_3$, (b) $[HGaNH]_4 \cdot 2NH_3$, and (c) $[HGaNH]_7 \cdot 2NH_3$. All distances are in angstroms, all angles in degrees. B3LYP/pVDZ level of theory.

for a GaN nanoparticle formation. To reduce the possibility of formation of liquid gallium metal, the process should be carried out at temperatures below 400 K. As recent experiments show,[26,27] laser irradiation is the best way to initiate the process of particle generation.

IV. Organometallic Substituents. As was shown before, thermodynamic data obtained for the H−Ga−N−H and CH_3−Ga−N−H systems are qualitatively very similar,[30,62] and therefore in the present work we have focused on hydrogen-containing systems, which are most amenable to theoretical studies. Results obtained for the hydrogen analogues can be extended to organometallic derivatives as well. To further support this contention, several small methyl-substituted substances have been investigated. Optimized structural parameters are given in Figure 10, and thermodynamic characteristics are summarized in Table 8, together with results for hydride derivatives.

Subsequent oligomerization enthalpies are very similar for H- and Me-containing species, so the small increase of bulkiness does not affect the thermodynamics of the oligomerization reactions. The energetics of imidogallane generation from $GaMe_3$ and ammonia are much more favorable compared to that from GaH_3 and ammonia. This suggests that it will be possible to achieve even higher oligomerization degrees for

(60) Afeefy, H. Y.; Liebman, J. F.; Stein, S. E. Neutral Thermochemical Data. In *NIST Chemistry WebBook*, NIST Standard Reference Database Number 69; Linstrom, P. J., Mallard, W. G., Eds.; National Institute of Standards and Technology: Gaithersburg MD, March 2003 (http://webbook.nist.gov).
(61) Ranade, M. R.; Tessier, F.; Navrotsky, A.; Leppert, V. J.; Risbud, S. H.; DiSalvo, F. J.; Balkas, C. M. *J. Phys. Chem. B* **2000**, *104*, 4060.
(62) Timoshkin, A. Y.; Bettinger, H. F.; Schaefer, H. F. *J. Phys. Chem. A* **2001**, *105*, 3240.

Table 8. Comparison of the Thermodynamic Characteristics for the Selected Reactions[a]

	R = H		R = CH_3	
process	ΔH^0_{298}	ΔS^0_{298}	ΔH^0_{298}	ΔS^0_{298}
$^1/_6$ $[RGaNH]_6 \rightarrow {}^1/_7$ $[RGaNH]_7$	−3.14	−5.27	−2.98	−4.87
$^1/_7$ $[RGaNH]_6 \rightarrow {}^1/_8$ $[RGaNH]_8$	−5.66	−3.26	−5.35	−4.77
$GaR_3 + NH_3 \rightarrow {}^1/_7$ $[RGaNH]_7 + 2HR$	−140.2	−67.4	−213.4	−86.5
$GaR_3 + NH_3 \rightarrow {}^1/_8$ $[RGaNH]_8 + 2HR$	−145.9	−70.7	−218.8	−91.3
$2[R_2GaNH_2]_3 \rightarrow [R_9Ga_6N_6H_9] + 3HR$	5.5	84.3	−97.9	78.9
$[R_2GaNH_2]_3 + GaR_3 + NH_3 \rightarrow [RGaNH]_4 + 5HR$	−13.3	192.1	−232.3	205.1
$[R_9Ga_6N_6H_9] + GaR_3 + NH_3 \rightarrow [RGaNH]_7 + 5HR$	−79.1	229.1	−327.9	294.9

[a] Standard enthalpies in kJ mol^{-1}, standard entropies in J mol^{-1} K^{-1}. B3LYP/pVDZ level of theory.

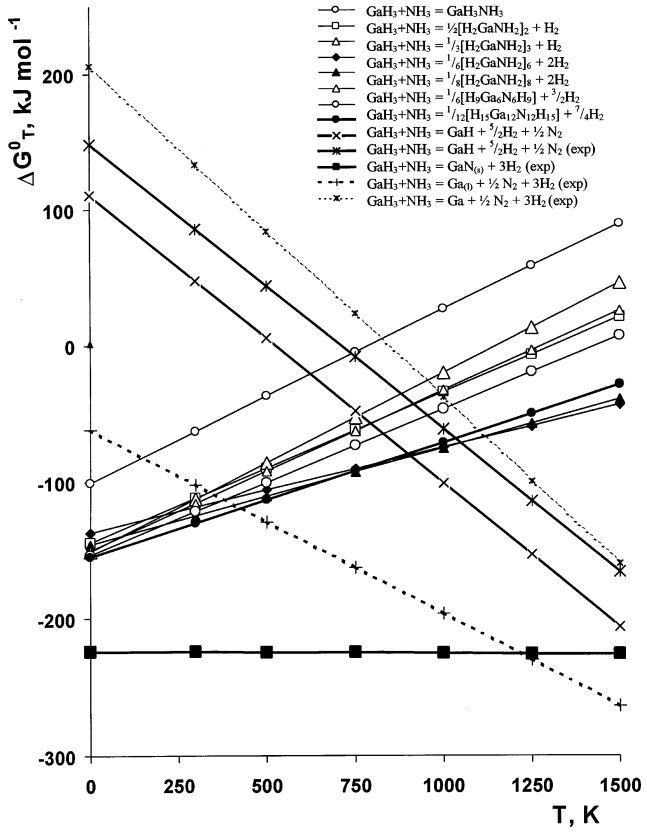

Figure 9. Gibbs energy−temperature diagram for GaN CVD from GaH_3 and ammonia.

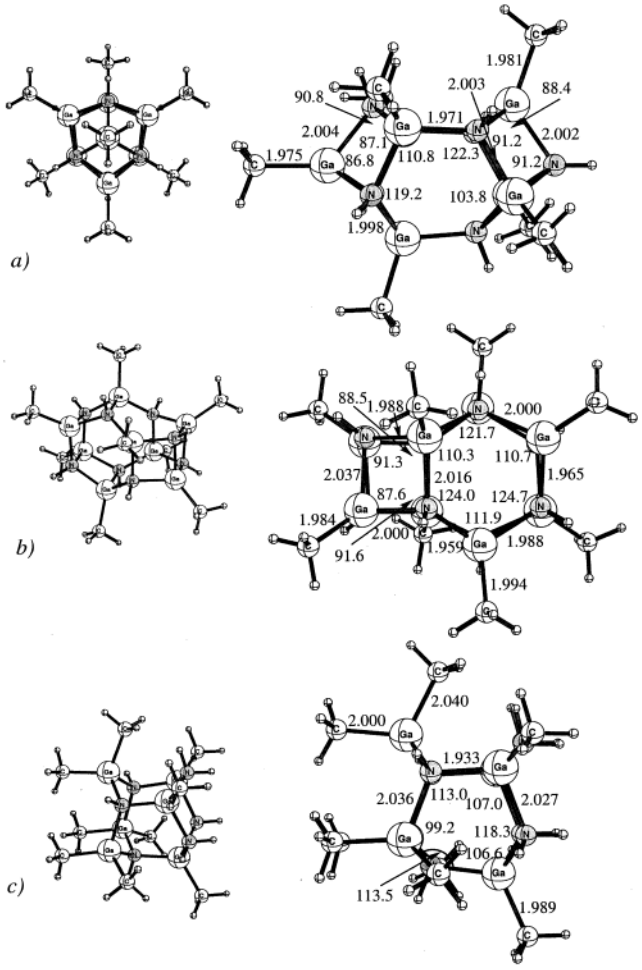

Figure 10. Optimized structural parameters of several Me-substituted compounds: (a) $[MeGaNH]_7$, (b) $[MeGaNH]_8$, and (c) $[Me_9Ga_6N_6H_9]$. All distances are in angstroms, all angles in degrees. B3LYP/pVDZ level of theory.

methyl-substituted imidogallanes. Dimerization of $[Me_2GaNH_2]_3$ with formation of $[Me_9Ga_6N_6H_9]$ is exothermic (in contrast to cyclotrigallazane), and the capping reactions to form needle-shaped imidogallanes are also much more favorable in the case of methyl substituents. Thus, all considered processes are more favorable for Me substituents compared to the unsubstituted species. Therefore, formation of large-mass oligomers in the $GaMe_3-NH_3$ system is very favorable thermodynamically under low-temperature/high-pressure conditions.

In the present report we have presented the results of a fairly comprehensive thermodynamic analysis. Detailed pathways for the formation of needle-shaped imido compounds also need to be investigated. However, the lower Ga−N bond energies in the clusters compared to those of Al−N facilitates the processes of interconversion of imidogallanes. Experimental and theoretical studies of the kinetics of elimination processes show that activation barriers are small (about 35−48 kJ mol^{-1}).[63,64] All these observations suggest that kinetic factors may not be limiting when the laser-assisted MOCVD process is carried out. In principle, laser irradiation brings to the system such an excess of energy that it overcomes all the possible barriers and reaches the thermodynamic sink. Therefore, the thermodynamic analysis presented here indicates a high probability of utilizing gas-phase association reactions for the generation of GaN nanoparticles.

Conclusions

We have shown that the needle-shaped imidogallanes with high oligomerization degrees possess greater stability than cage structures. We propose that this result can be generalized to

(63) Alwan, J. J.; Eden, J. G. *Chem. Vap. Deposition* **1997**, *3*, 209.

(64) Makino, O.; Nakamura, K.; Tachibana, A.; Tokunaga, H.; Akutsu, N.; Matsumoto, K. *Appl. Surf. Sci.* **2000**, *159*, 374.

the analogous clusters of the main group elements. Thus, the "isolated square rule", which is analogous to the "isolated pentagon rule" widely applied for fullerenes, should not serve as the basis for the search for the most stable structures.

Generation of gas-phase imidogallanes is very favorable thermodynamically starting both from GaH_3 and ammonia and from cyclotrigallazane. Spontaneous growth of needle-shaped oligomers in the gas phase is expected under low-temperature conditions. It is argued that their subsequent nucleation will lead to the formation of GaN nanoparticles.

Amido-imido compounds, formed by fusion of Ga_3N_3 rings, appear to be suitable intermediates for the growth of needle structures. Their capping energies are greatly enhanced with the increase of the oligomerization degree *n*. At low temperatures, reaction of needle-shaped clusters with ammonia, leading to the formation of adamantane-type structures, is also favorable thermodynamically. It is expected that the stability of such "ammonia uptake" structures will decrease with oligomerization degree. A case study of methyl-substituted oligomers shows that the results may be generalized to organometallic precursors as well.

Considering the well-known analogy between Ga−N, Al−N, Ga−O, Al−O, and Ga−S based structures, the results obtained in the present study suggest that large needle-shaped oligomers may be important for other 13−15, as well as the analogous 13−16 compounds.

Acknowledgment. A.Y.T. is grateful to the Alexander-von-Humboldt Foundation for a research fellowship and for a return fellowship. The hospitality of the Philipps-Universität Marburg (Prof. Gernot Frenking) is especially appreciated. Financial support from the Educational Ministry of Russian Federation and the St. Petersburg Administration (Grant PD03-1.3-117) is gratefully acknowledged. Work at the University of Georgia was supported by the NSF Grant CHE-0136186.

Supporting Information Available: Selected structural parameters for all investigated imido compounds, harmonic vibrational frequencies and IR intensities for investigated compounds, and details on the estimation of the standard enthalpy of formation of GaH_3(g). This material is available free of charge via the Internet at http://pubs.acs.org.

JA0400483